UNIVERSIDAD DISTRITAL
FRANCISCO JOSÉ DE CALDAS

Revista Científica

http://revistas.udistrital.edu.co/ojs/index.php/revcie/index

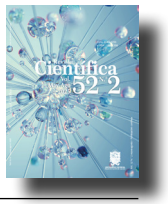

Artículo de investigación científica

Detección de asbesto-cemento en imágenes hiperespectrales a partir de la aplicación de la similitud de fase de Fourier

Detection of Asbestos-Cement in Hyperspectral Images Based on the Application of Fourier Phase Similarity

Detecção de amianto-cimento em imagens hiperespectrais com base na aplicação da similaridade de fase de Fourier

Gabriel Elías Chanchí-Golondrino[1]
Manuel Alejandro Ospina-Alarcón[2]
Manuel Saba[3]

Recibido: 7 de marzo de 2025 **Aceptado:** 28 de octubre de 205

Para citar este artículo: Chanchí-Golondrino, G. E., Ospina-Alarcón, M. A. y Saba, M. (2025). Detección de asbesto-cemento en imágenes hiperespectrales a partir de la aplicación de la similitud de fase de Fourier. *Revista Científica*, *52*(2), 21-37. https://doi.org/10.14483/23448350.23314

Resumen

Uno de los desafíos en el campo de las imágenes hiperespectrales es la identificación de métodos para la detección eficaz y eficiente de materiales, en vista de la alta dimensionalidad de los datos asociados a los cientos de bandas de reflectancia. En este sentido, dada la regulación en cuanto al uso de asbesto en la construcción y las implicaciones de este material para la salud humana, ha cobrado relevancia la teledetección. En este trabajo se propone un nuevo enfoque computacional para la detección de asbesto-cemento que utiliza la similitud de fase entre la representación espectral de Fourier del pixel característico y la de las demás firmas espectrales en la imagen. Para el desarrollo de esta investigación, se adaptó la metodología CRISP-DM. A manera de resultado, se implementó el enfoque propuesto en una imagen hiperespectral del barrio Manga de la ciudad de Cartagena de Indias (Bolívar, Colombia). El porcentaje de asbesto detectado por medio de nuestro método difiere en un 1.74 % con respecto al tradicional método de correlación. Asimismo, el enfoque propuesto demostró ser 0.86 % más eficiente que este último. De acuerdo con los resultados obtenidos, nuestro enfoque se constituye en una alternativa competitiva, siendo de gran utilidad en escenarios que involucren imágenes de gran cobertura y requieran optimizar el tiempo de procesamiento. Dado el uso de tecnologías de código abierto, este enfoque puede ser extrapolado fácilmente en el dominio académico y empresarial con el fin de detectar asbesto-cemento y otros materiales.

Palabras clave: imágenes hiperespectrales, detección de asbesto-cemento, sensado remoto, similitud de fase, transformada rápida de Fourier

1. Full professor of the Faculty of Engineering of Universidad de Cartagena, Cartagena de Indias, Colombia, email: gchanchig@unicartagena.edu.co
2. Full professor of the Faculty of Engineering of Universidad de Cartagena, Cartagena de Indias, Colombia email: mospinaa@unicartagena.edu.co
3. Full professor of the Faculty of Engineering of Universidad de Cartagena, Cartagena de Indias, Colombia, email: msaba@unicartagena.edu.co

Abstract
One of the challenges in the field of hyperspectral imaging is identifying methods for the effective and efficient detection of materials, given the high dimensionality of the data associated with hundreds of reflectance bands. In this regard, given the regulations on the use of asbestos in construction and the implications of this material for human health, remote sensing has become increasingly important. This paper proposes a new computational approach for the detection of asbestos-cement that uses the phase similarity between the Fourier spectral representation of the characteristic pixel and that of the other spectral signatures in the image. The CRISP-DM methodology was adapted for the development of this research. As a result, the proposed approach was implemented on a hyperspectral image of the Manga neighborhood in the city of Cartagena de Indias (Bolívar, Colombia). The percentage of asbestos detected using our method differs by 1.74% from the traditional correlation method. Likewise, the proposed approach proved to be 0.86% more efficient than the latter. Based on the results obtained, our approach is a competitive alternative, being very useful in scenarios involving large-coverage images and requiring optimized processing time. Given the use of open-source technologies, this approach can be easily extrapolated in the academic and business domains to detect asbestos-cement and other materials.
Keywords: hyperspectral imaging, asbestos-cement detection, remote sensing, phase similarity, fast Fourier transform

Resumo
Um dos desafios no campo das imagens hiperespectrais é a identificação de métodos para a detecção eficaz e eficiente de materiais, tendo em vista a alta dimensionalidade dos dados associados às centenas de bandas de refletância. Nesse sentido, dada a regulamentação sobre o uso do amianto na construção e as implicações desse material para a saúde humana, a teledeteção ganhou relevância. Neste trabalho, propõe-se uma nova abordagem computacional para a detecção de amianto-cimento que utiliza a similaridade de fase entre a representação espectral de Fourier do pixel característico e a das demais assinaturas espectrais na imagem. Para o desenvolvimento desta pesquisa, foi adaptada a metodologia CRISP-DM. Como resultado, a abordagem proposta foi implementada numa imagem hiperespectral do bairro Manga da cidade de Cartagena de Indias (Bolívar, Colômbia). A porcentagem de amianto detectada por meio do nosso método difere em 1,74% em relação ao método tradicional de correlação. Além disso, a abordagem proposta mostrou ser 0,86% mais eficiente que este último. De acordo com os resultados obtidos, nossa abordagem constitui uma alternativa competitiva, sendo de grande utilidade em cenários que envolvem imagens de grande cobertura e exigem a otimização do tempo de processamento. Dado o uso de tecnologias de código aberto, essa abordagem pode ser facilmente extrapolada no domínio acadêmico e empresarial com o objetivo de detectar amianto-cimento e outros materiais.
Palavras-chaves: imagens hiperespectrais, detecção de cimento-amianto, sensoriamento remoto, similaridade de fase, transformada rápida de Fourier

INTRODUCTION

Remote sensing, also known as *teledetection*, can be defined as a technology that allows acquiring information about objects or surface characteristics of the Earth without direct contact, utilizing electromagnetic radiation as the medium of interaction (Awange & Kiema, 2019; Fu *et al.*, 2020). To this effect, sensors and other instruments deployed on spaceborne, airborne, or terrestrial platforms are used, capturing their interaction with surface objects or materials in terms of reflectance, emission, or absorption, which in turn allows characterizing the physical and chemical properties of land cover (Jiménez-López *et al.*, 2015). Unlike traditional methods, which can be destructive and require significant time for data collection, remote sensing is non-invasive and enables rapid data acquisition, which is crucial, for instance, in applications such as soil property measurement and wildfire monitoring (Fang, 2024). In this context, remote sensing allows for the simultaneous observation of large areas of the Earth's surface, making it highly valuable for natural resource management and disaster monitoring (Navalgund *et al.*, 2007; Wang *et al.*, 2022).

Within the widespread development of artificial intelligence (AI), one of the most prominent topics is computer vision (Akinlade *et al.*, 2023; Taiwo *et al.*, 2025). In the context of remote sensing, this area of knowledge has been applied to the analysis of hyperspectral images, namely spectral datacubes or three-dimensional data structures composed of two spatial dimensions (x, y) and one spectral dimension (λ) (Ruiz Guzmán *et al.*, 2024). This enables the simultaneous capture of images across multiple wavelengths, allowing for a detailed multivariate analysis of the structural, molecular, and functional properties of the observed objects or materials (Burger & Gowen, 2011; Gao & Smith, 2015; Liu *et al.*, 2021). Unlike multispectral imaging, hyperspectral images offer a high spatial resolution, as they capture a continuous spectrum with hundreds of bands, thereby enabling a more precise identification of materials and objects (Muhammed *et al.*, 2020; Ortega *et al.*, 2019).

Regarding asbestos-cement detection, various studies have been conducted, in light of the effects of asbestos on public health, particularly concerning the respiratory diseases that arise in individuals exposed to this material (Z. Jiang *et al.*, 2022; Musk *et al.*, 2020; Ospina *et al.*, 2019). In this regard, hyperspectral imaging in the shortwave infrared range (SWIR; 1000-2500 nm) has been employed to detect and classify asbestos-cement minerals such as amosite, crocidolite, and chrysotile in cement matrices, using techniques such as principal component analysis (PCA) and soft independent modeling of class analogies (SIMCA) for material sample classification, achieving high specificity and sensitivity (Bonifazi *et al.*, 2015, 2018). Additionally, in Bassani *et al.* (2007), a systematic procedure was developed to recognize and assess the deterioration of asbestos-cement roofs, utilizing hyperspectral data and linear regression analysis to estimate the abundance of asbestos fibers on the surface. Moreover, multivariate classification methods, including partial least squares discriminant analysis (PLS-DA) and support vector machines (SVM), were used to recognize and classify asbestos-cement in construction and demolition waste, showcasing these methods' potential for rapid and reliable quality control strategies (Bonifazi *et al.*, 2019, 2022). Similarly, in Krówczyńska *et al.* (2020), hyperspectral imaging and convolutional neural networks were used to identify asbestos-cement roofs in aerial photographs, achieving an accuracy of 89%.

As for the challenges identified in hyperspectral imaging, the high dimensionality of the resulting images stands out due to the hundreds of spectral bands used, which implies high computational complexity and hinders the efficient processing of information (Hu *et al.*, 2024; Plaza *et al.*, 2009). In this regard, hyperspectral image classification methods, such as those based on deep learning, are widely employed due to their effectiveness. However, they require a significant amount of computational resources, as deep neural networks must be trained with large volumes of data (Li *et al.*, 2019; Sifnaios *et al.*, 2024).

Thus, given the high dimensionality of the data, material classification algorithms must be capable of efficiently handling large volumes of information (Enríquez Aguilera *et al.*, 2018). Based on the above, dimensionality reduction methods (*e.g.*, PCA) have been widely adopted to reduce the dimensionality of spectral data without losing essential information, thereby improving the efficiency of processing algorithms (Asghari Beirami & Mokhtarzade, 2020; J. Jiang *et al.*, 2018; Zhang *et al.*, 2022). In this vein, one of the challenges in the field of hyperspectral imaging is the identification of new methods that aid in mitigating the computational cost of processing while achieving results comparable to those obtained through more complex or widely used techniques.

The main motivation of this work was to evaluate the feasibility, in terms of effectiveness and efficiency, of a new approach for detecting asbestos-cement in hyperspectral images using Fourier phase similarity, with the aim of identifying alternatives to methods based on spectral distance and machine learning. As a contribution, this article proposes the application of a novel computational approach for detecting asbestos-cement in hyperspectral images, which is based on the phase similarity between the fast Fourier transform (FFT) of the characteristic pixel of asbestos-cement and the Fourier transform of the remaining pixels in the image. The FFT can be defined as an algorithmic method that efficiently computes the discrete Fourier transform (DFT) of a data series. It is significantly faster than the direct approaches for calculating the DFT, which makes it particularly useful and suitable for signal analysis (Brigham & Yuen, 1978; Gan, 2020; Pollard, 1971), wherein it is widely used, enabling the conversion of signals from the time domain to the frequency domain, and *vice versa*. This is beneficial for analyzing and processing signals that may be complex in the time domain (Baker, 2003; Gan, 2020; Kollar *et al.*, 2018). The proposed approach was initially evaluated using a sample of spectral signatures of asbestos-cement and other materials across different spectral band ranges, which were obtained from a reference hyperspectral image of the Manga neighborhood in the city of Cartagena, with dimensions of 725 × 850 pixels and 380 reflectance bands. This evaluation sought to determine the predictive capacity of the method in each reflectance band range, as evidenced by the difference between the minimum phase similarity to spectral signatures of vegetation and the maximum similarity to signatures of other materials. Furthermore, using the best detected threshold, the proposed approach was deployed over the entire reference image in order to determine its percentage of asbestos-cement and compare it against the value detected via the correlation method, which has been widely used for material detection in hyperspectral images (Chanchí Golondrino *et al.*, 2023). In addition, the computational efficiency of the approach was compared to that of the correlation method by executing multiple repetitions over a selected region of the reference hyperspectral image. The proposed approach was first evaluated by calculating the minimum and maximum similarity of the spectral signature with respect to the selected sample signatures across different wavelength ranges, verifying the absence of overlap. Likewise, when deploying the proposed approach over the complete image, its effectiveness was assessed through the visual inspection of misclassified pixels. On the other hand, the relative computational efficiency was determined by comparing the processing times of our approach against those of the correlation method over a subregion of the image across multiple repetitions.

The results obtained regarding efficacy and efficiency led to the conclusion that our proposal is a competitive alternative for integration into remote sensing-based monitoring systems for asbestos-cement and other materials. Likewise, given our use of libraries and technologies for implementation, our method can be extrapolated, hybridized, and replicated in both academic and industrial contexts involving experimentation with spectral images, serving as an alternative to proprietary tools. Moreover, the results obtained regarding the percentage of asbestos-cement in one of the most representative neighborhoods of Cartagena are of great interest to governmental authorities, considering their implications for public

health due to respiratory diseases (Algranti *et al.*, 2001; Durán-Ávila *et al.*, 2021; Mainieri Hidalgo *et al.*, 2009; Musk *et al.*, 2020). Finally, it is worth highlighting that the three main contributions of this research lie in a) our assessment of the feasibility of applying the Fourier phase similarity approach for asbestos-cement detection in hyperspectral images, b) the identification of the wavelength ranges in which the proposed approach does not exhibit overlap in asbestos identification, and c) the effectiveness and efficiency achieved by our proposal when compared to the spectral correlation method.

The remainder of this article is organized as follows. The methodology section presents the phases of this research. The results section includes the computation of the FFT of the characteristic asbestos-cement pixel across different reflectance band ranges, the evaluation of the phase similarity between the transforms of the characteristic pixel and those of sample pixels of asbestos-cement and other materials across different band ranges, the deployment of the proposed approach over the entire hyperspectral image using the best detected thresholds, and the assessment of the efficacy and efficiency of our proposal compared to the spectral correlation method. Finally, the conclusions drawn from this research are presented, as well as potential avenues for future work.

METHODOLOGY

In this research, the CRISP-DM data science methodology was adapted into four phases:

- P1 – Business and data understanding
- P2 – Data preparation
- P3 – Modeling and evaluation
- P4 – Deployment

This methodology was selected since it is a widely used standard model for the development of data mining projects, which is characterized by its independence of the industrial sector and of the technology employed, allowing for applications across a wide variety of contexts and projects (Abasova *et al.*, 2021; Hayat Suhendar & Widyani, 2023; Martinez-Plumed *et al.*, 2021; Nava & Hernández, 2012).

Figure 1. *Adaptation of the CRISP-DM methodology*

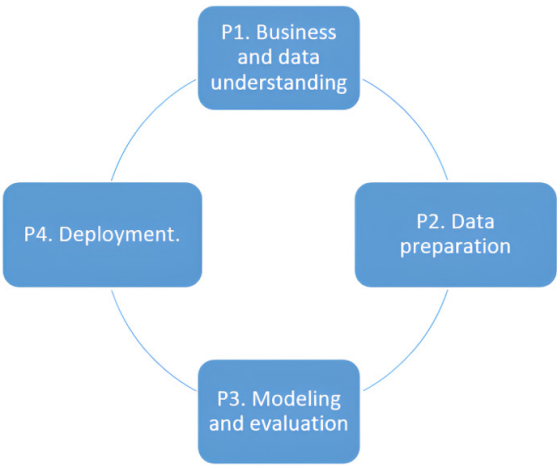

In P1, a total of 75 spectral signatures of asbestos-cement, as well as and 75 signatures of other materials, were obtained from a reference hyperspectral image of the Manga neighborhood in the city of Cartagena de Indias (Bolívar, Colombia), with a total resolution of 725 × 850 pixels and 380 reflectance bands. This image underwent the corresponding atmospheric corrections to ensure the accuracy of the surface reflectance values. This resolution was selected to evaluate the detection thresholds and the reflectance bands in which the proposed approach allows differentiating asbestos-cement from other materials. Figure 2 presents, within an RGB representation of the hyperspectral image, the 75 selected asbestos-cement sample pixels (blue) and the 75 pixels of other materials (red). Among the latter, spectral signatures of water, vegetation, roads, and other surfaces were selected through visual inspection.

Figure 2. *Selected sample pixels of asbestos-cement and other materials*

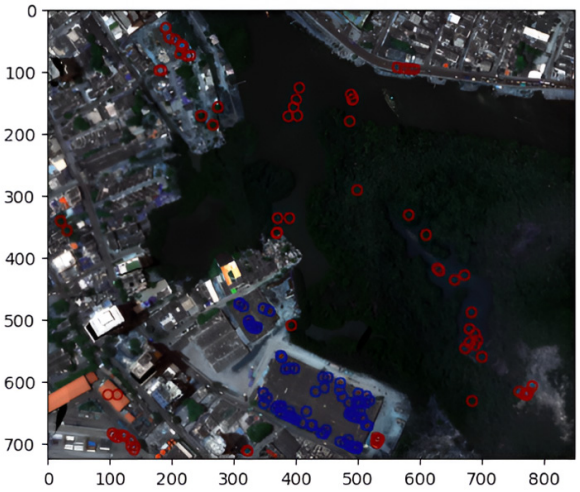

Afterwards, in P2, normalization was performed based on the 75 asbestos-cement sample pixels, and their characteristic pixel (or the average asbestos-cement pixel) was obtained by computing the mean reflectance for each spectral band across all pixels and spectral signatures. Figure 3 presents both the sample spectral signatures (left side) and the computed average pixel (right side).

Figure 3. *Sample pixels and the average pixel of asbestos-cement*

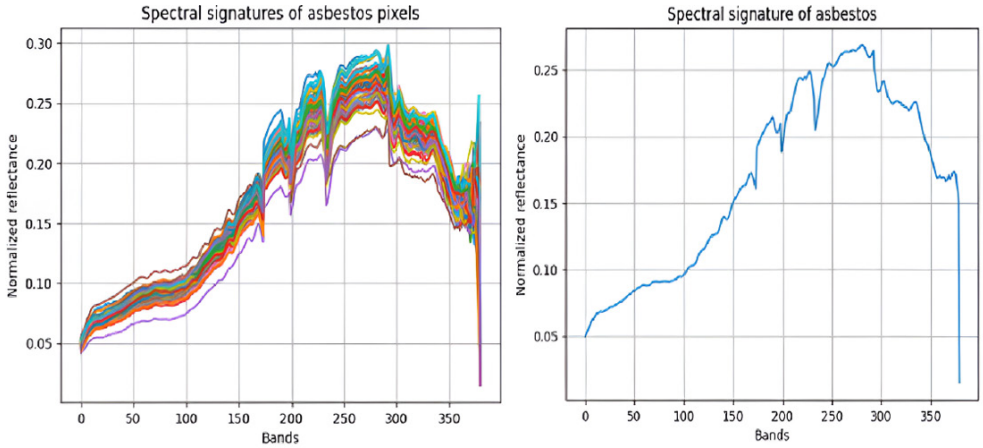

Similarly, based on the characteristic spectral signature of asbestos-cement, the FFT of the average pixel was computed, obtaining a spectral representation that was used for comparison with the spectral representations of the sample pixels, in order to identify their similarity to the pixels of asbestos-cement and other materials.

In P3, the proposed approach, based on the Fourier phase similarity, was implemented and evaluated using all sample pixels. Through the 380 reflectance bands, the phase similarity between the spectral representation of the average pixel and those of the two sample groups was determined, aiming to establish the minimum threshold at which the proposed approach successfully differentiates the spectral signature of asbestos-cement. It should be noted that, in order to calculate the Fourier phase similarity, we employed Equation (1).

$$PhaseSim = \frac{1}{N}\sum_{k=1}^{N} e^{j\left(\arg\left(Y_1[k]\right) - \arg\left(Y_2[k]\right)\right)} \tag{1}$$

Here, Y_1[k] corresponds to the FFT of the characteristic or average pixel, Y_2[k] represents the FFT of a specific pixel in the hyperspectral image, and arg(Y[k]) denotes the phase of the k-th component in the Fourier domain. Since the pixels in the hyperspectral image contained 380 reflectance bands, the default value of N = 380 was used. However, depending on the detection capability of the proposed approach, a subset of these bands may be selected. Similarly, the magnitude of the Fourier phase similarity was determined using Equation (2).

$$Mag.PhaseSim = \sqrt{\left(Re\left(PhaseSim\right)\right)^2 + \left(Im\left(PhaseSim\right)\right)^2} \tag{2}$$

Equations (1) and (2) were implemented using the *NumPy* library in Python, employing both the FFT method and operations with numerical arrays. It should be noted that, in the event of an overlap between the minimum similarity to asbestos-cement pixels and the maximum similarity to pixels of other materials, the process returned to P2, where a subset of the 380 bands was selected to compute a new average pixel and its FFT, as well as the detection thresholds for this specific set of bands. This ensured the identification of the band range in which the proposed approach can effectively detect asbestos-cement.

Finally, once the appropriate detection thresholds for asbestos-cement had been identified, P4 proceeded with the deployment of the proposed approach over the entire reference image, aiming to determine the percentage of asbestos-cement pixels within it and compare this value against that obtained using the correlation method, one of the most widely used approaches for material detection in hyperspectral images. In this context, and in order to evaluate the computational efficiency of our proposal *vs.* the aforementioned method, 25, 50, 75, and 100 executions were performed to obtain the average processing time for each one—as well as the total average—, which allowed determining the relative efficiency of our proposal.

RESULTS

To obtain the results, the first step involved applying the FFT to the average pixel in order to obtain the spectral representation of asbestos-cement, which would be processed by means of its phase similarity to the spectral representation of other pixels. Figure 4 presents both the average asbestos-cement pixel (left side) and its Fourier spectral representation (right side).

Figure 4. *Average asbestos pixel and its Fourier spectral representation*

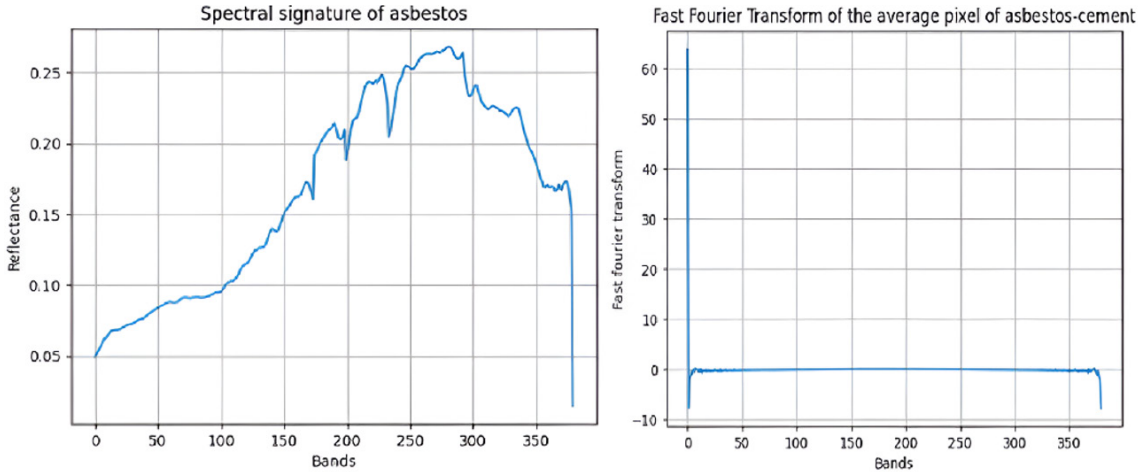

Although a large number of zero values can be observed within the Fourier spectral representation of the characteristic signature, this behavior is normal and expected in hyperspectral signals, as most of their energy is concentrated at low frequencies due to the continuous and smooth nature of spectral variations between consecutive bands. Using the spectral representation from Figure 4, Equations (1) and (2) were applied to compute the phase similarity to the sample pixels of asbestos-cement and other materials, utilizing the 380 bands of the original image. This process resulted in the minimum and maximum similarity values presented in Figure 5.

Figure 5. *Phase similarity obtained with the sample pixels in 380 bands*

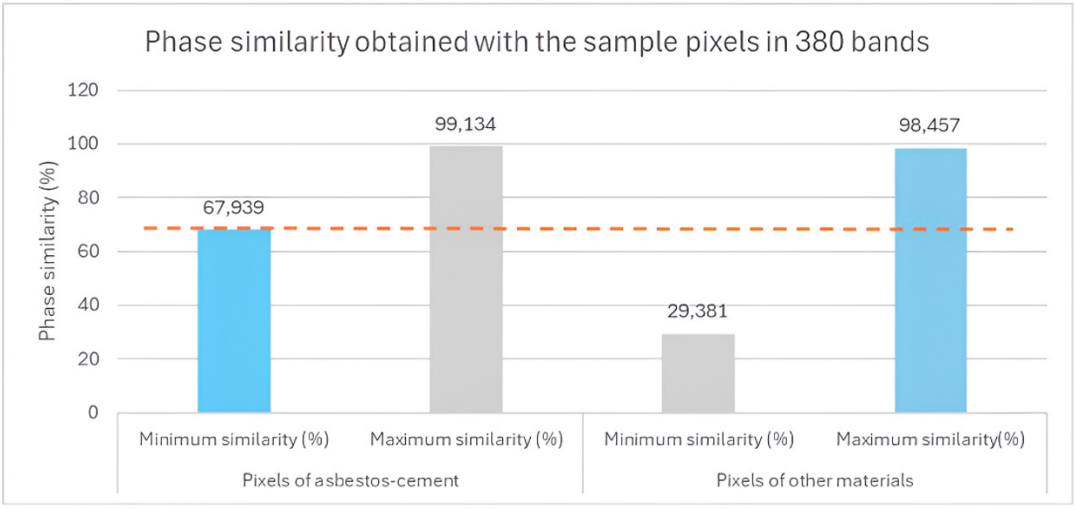

According to these results, there is an evident overlap between the minimum similarity to asbestos-cement pixels and the maximum similarity to other materials, indicating that the proposed approach does not adequately detect asbestos-cement when using all 380 reflectance bands. Therefore, it is necessary to identify the most relevant bands. To this effect, different methods were programmed in Python, using the *NumPy* library to progressively iterate through different band ranges, *i.e.*, 0 to 380, 100 to 380, and

150 to 300, identifying the bands with a positive difference between the minimum similarity to asbestos-cement pixels and the maximum similarity to other materials. The selection of the 100 to 380 and 150 to 380 ranges was based on the fact that, in these ranges, the spectral signature of asbestos-cement exhibits significant peaks, which may facilitate its differentiation from other pixels in the Fourier spectral domain. Consequently, Figure 6 presents the five band ranges that achieved the highest difference, meaning those in which the proposed approach enables the adequate differentiation between asbestos-cement and other materials.

Figure 6. *Difference of similarities across spectral band ranges*

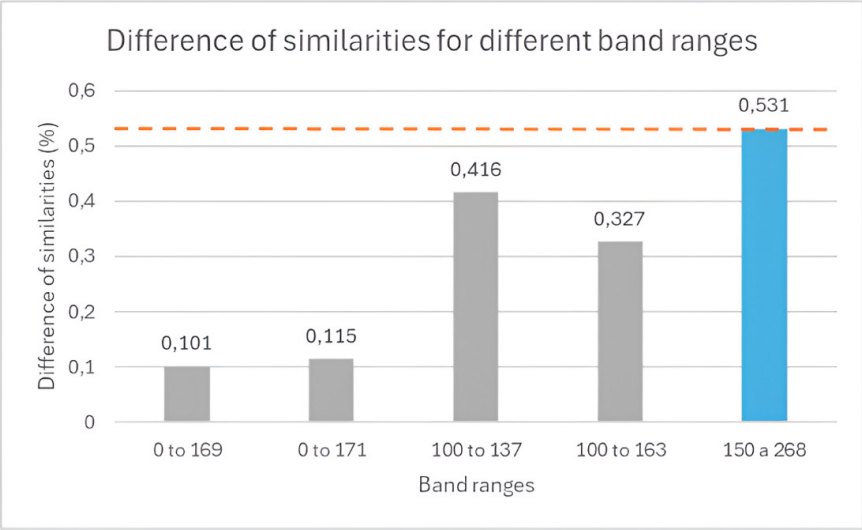

As shown in this Figure, the band range that allows for the greatest differentiation between pixels of asbestos-cement and other materials via the proposed approach is 150 to 268, with a percentage difference of 0.531. The 0 to 137 range is also noteworthy, with a percentage difference of 0.416. With this information, and considering the best-performing band range, the average asbestos-cement pixel and its associated FFT were recalculated (Figure 7).

Figure 7. *Fourier transform of the characteristic pixel in the 150 to 268 range*

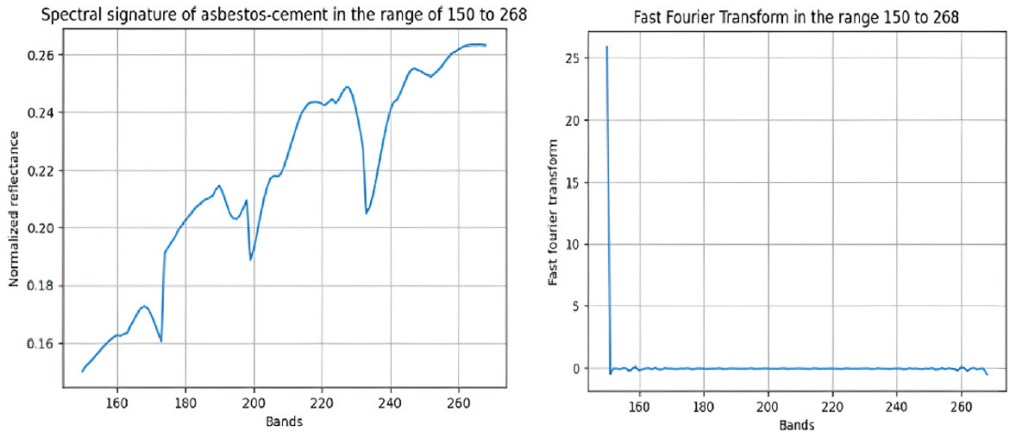

Thus, based on the spectral representation of asbestos-cement for the specified band range, the proposed approach was deployed over the entire reference image, considering that, for this range, the minimum similarity percentage required to detect asbestos-cement is 97.106%. Figure 8 presents both the implementation of the proposed approach over the entire reference image of the Manga neighborhood and the detected asbestos-cement areas, which are highlighted in blue.

Figure 8. *Implementation of the proposed approach on the reference image*

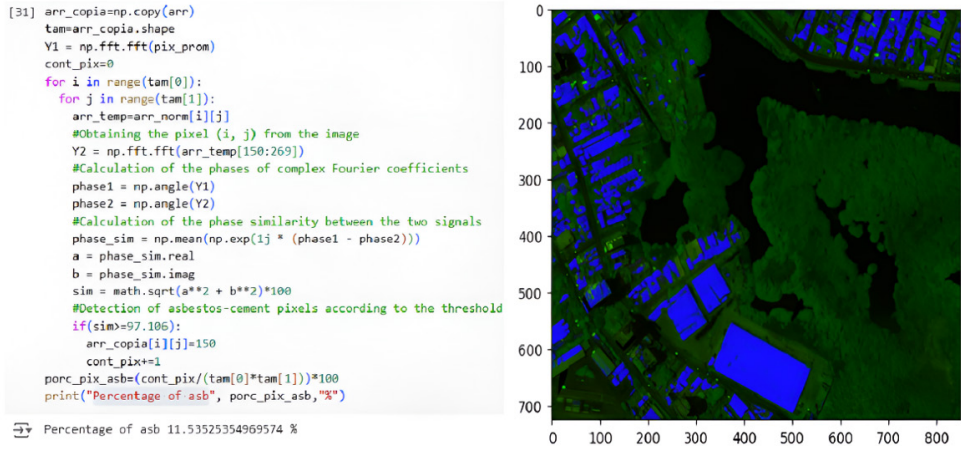

Note that, for the implementation of our method, an iteration was performed over the *NumPy*-based datacube, which represents the hyperspectral image and was obtained via the *Spectral* library. For each pixel, the Fourier spectral representation (Y_2) was computed using the *fft()* method from the *NumPy* library. Subsequently, the phase similarity was calculated with respect to the Fourier spectral representation of the characteristic pixel (Y_1), after which the pixels whose similarity to the average was equal to or greater than 97.106% were classified and colored blue. In this case, the percentage of asbestos-cement pixels detected in the reference image was 11.53%. Furthermore, to assess whether the effectiveness of the proposed approach was similar or superior to that of the correlation method, the latter was also implemented on the reference image (Figure 9).

Figure 9. *Implementation of the correlation method on the reference image*

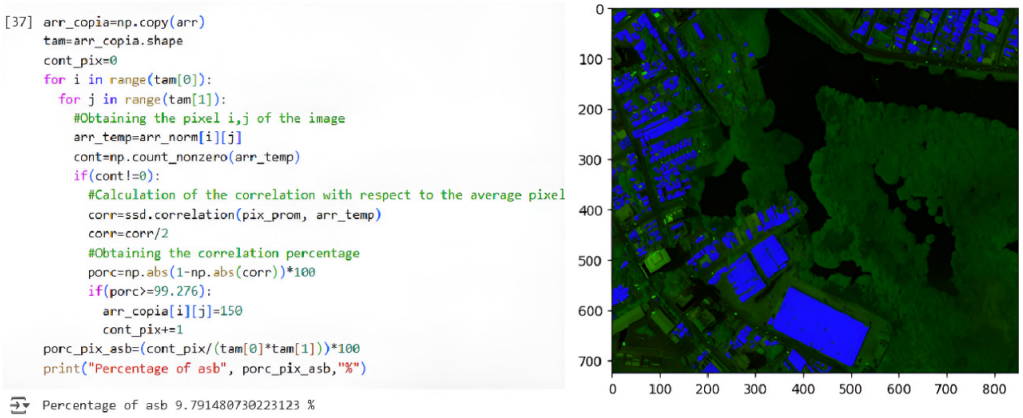

Note that the correlation method detected 9.79% of the asbestos-cement pixels in the reference hyperspectral image, while the proposed approach identified 1.74% more. Given that this difference is relatively small, it can be said that both methods have comparable effectiveness. This comparison is further illustrated in Figure 10, which presents the results of the best-performing variants of the proposed approach relative to the correlation method. It is worth noting that the spectral correlation method was not evaluated across different wavelength ranges, since it exhibits no similarity overlap across all image bands.

According to the results presented in Figure 10, the percentage of asbestos-cement detected by the different variants of the proposed approach, *i.e.*, the method implemented across different band ranges, varies between 10.97 and 12%, with a maximum difference of 2.21% compared to the correlation method and a minimum difference of 1.18%. This leads to the conclusion that, although the proposed approach demonstrates the greatest differentiation capability when applied to the 150 to 268 band range, the variants corresponding to the band ranges considered in Figure 6 are also comparable to the correlation method in terms of effectiveness.

Figure 10. *Comparison between our method's variants and the correlation method in asbestos-cement detection*

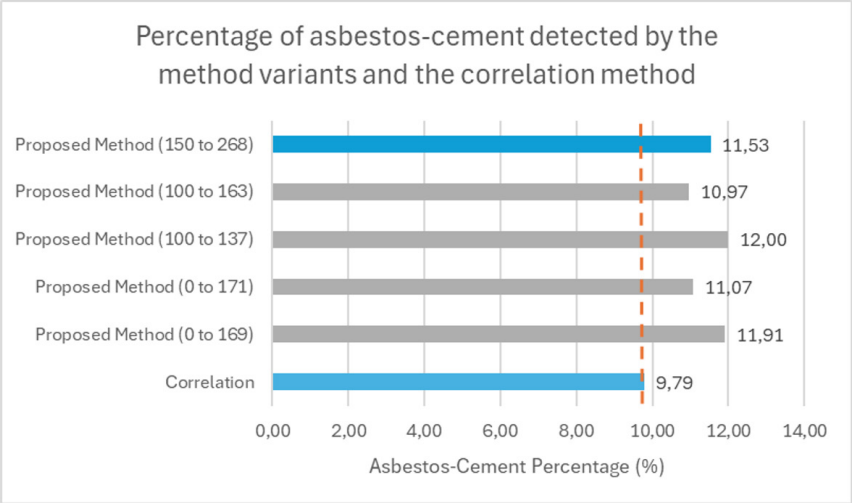

Finally, to evaluate the computational efficiency of the variant with the greatest difference (150 to 268 bands) compared to the correlation method, multiple executions of both methods (25, 50, 75, and 100) were performed on a 20 × 20 region of the image with 380 reflectance bands. This process sought to compare the average processing time per execution as well as the total average, in order to determine the relative efficiency. It should be noted that the multiple executions of the methods were carried out using the *timeit* library in Python, which allows for multiple executions of a function while determining the total processing time. Figure 11 presents the results obtained for each method across different executions.

For 50, 75, and 100 repetitions, the correlation method exhibits slightly higher processing times compared to the proposed approach, with an average difference of 0.006 ms. Furthermore, when comparing the total average processing time of both methods, our proposal is, on average, 0.86% more efficient than the correlation method, meaning that the latter is 1.01 times slower. Therefore, given the minor efficiency difference between both methods, the proposed approach can be considered comparable to the correlation method, which makes it a valid alternative for deployment in material monitoring systems based on remote sensing.

Figure 11. *Average processing times by number of executions*

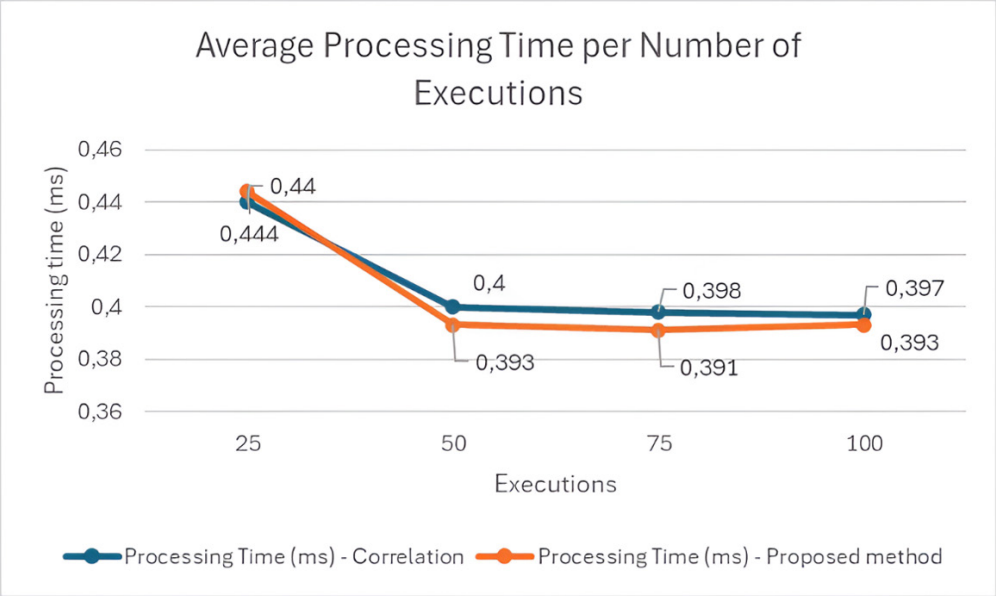

DISCUSSION

Given the need for computational methods that provide similar effectiveness to widely used approaches while being more efficient in terms of processing, this article proposes a novel approach for the detection of asbestos-cement which utilizes the Fourier phase similarity between the Fourier spectral representation of the characteristic pixel and that of different spectral signatures in an image. In this regard, it should be noted that our proposal demonstrated greater effectiveness in detecting this material within the 150 to 268 reflectance band range, detecting a slightly higher percentage of asbestos-cement pixels compared to the correlation method. Likewise, in terms of computational efficiency, the proposed approach proved to be slightly better than the correlation method, being 0.86% more efficient. This positions our proposal as a competitive alternative that can be extrapolated to research studies where the correlation method has been used for material detection, as in Chanchí Golondrino *et al.* (2023), where a comparison of different distance- and correlation-based methods for vegetation detection was conducted.

On the other hand, regarding studies involving the application of the Fourier transform for material detection in hyperspectral images, the proposed approach was more effective within the 150 to 268 band range, achieving a pixel differentiation capacity of 0.531% between pixels of asbestos-cement and other materials. In contrast, in Chanchí-Golondrino *et al.* (2024), where Fourier phase similarity was applied for vegetation detection, a differentiation capacity of 0.55% was achieved using the entire set of reflectance bands. This suggests that, across the 380 reflectance bands of the tested dataset, the proposed approach encountered fewer difficulties in identifying the spectral signature of vegetation compared to that of asbestos-cement. However, once the relevant bands had been filtered, the differentiation capacity became similar. In this regard, when applying this approach for the identification of other materials, it is essential to evaluate different band ranges in order to determine the most effective subset, allowing the method to achieve optimal differentiation.

Finally, it is noteworthy that this research utilized open-source libraries and technologies for both image processing and computational implementation. This represents a significant and competitive contribution to the field of asbestos-cement detection, and, given the promising results, the proposed approach can be extrapolated to the identification of other materials, standing as an open-source alternative to proprietary studies that rely on tools such as ENVI for hyperspectral image analysis (Sabah Jaber, 2018; Xing & Gómez, 2001). In this regard, our work provides a competitive advantage for research centers and universities in developing countries when it comes to experimenting with hyperspectral images, allowing them to replicate, extrapolate, customize, and hybridize the proposed approach for detecting different materials. This, in turn, offers a broader range of possibilities compared to those provided by proprietary tools for hyperspectral image analysis and processing.

CONCLUSIONS

Considering that one of the challenges in the field of remote sensing, particularly in material detection using hyperspectral images, is the identification of methods that enable effective detection while efficiently processing large volumes of spectral information derived from the hundreds of bands that compose these images, this article presents a novel computational approach based on the phase similarity between the Fourier spectral representations of the characteristic signature of asbestos-cement and the spectral signatures of pixels in an image. Compared to the correlation method, one of the most widely used techniques in remote sensing, the proposed approach achieved similar effectiveness and slightly superior computational efficiency, which makes it a competitive alternative for detecting asbestos-cement and other materials in hyperspectral images. Likewise, given the observed computational efficiency, this method may prove very useful in scenarios where, in addition to handling hundreds of spectral bands, there is extensive geographic coverage, as in environmental monitoring applications.

The proposed approach demonstrated a greater ability to differentiate between asbestos-cement and other materials within the 150 to 268 band range, as an overlap was observed between the minimum similarity to the asbestos-cement pixel sample and the maximum similarity to other materials when using all 380 bands. Thus, within the selected band range, our method determined an asbestos-cement percentage of 11.53% over the entire reference image, differing by 1.74% from the correlation method. It should be noted that this result was obtained by subtracting the percentage of asbestos-cement detected by the proposed approach over the entire image (11.53%) from that detected using the spectral correlation method (9.79%). Since this difference is not significant, the proposed approach can be considered comparable to the correlation method and regarded as a valid alternative for material detection in the field of hyperspectral imaging. Furthermore, it is important to note that, if the proposed approach is extrapolated to the detection of other materials, it is necessary to identify the representative bands in which it enables greater material differentiation.

In evaluating the computational efficiency of the proposed approach compared to the correlation method, multiple executions were performed for both methods on a 20 × 20 pixel region of the reference image, with 380 reflectance bands, utilizing the advantages provided by Python's *timeit* library. The results indicated that the proposed approach is 0.86% more efficient than the correlation method. Although this improvement in efficiency is minor, the proposed approach could be highly useful in fields such as environmental monitoring, where hyperspectral images not only contain hundreds of spectral bands but also cover large geographic areas. In such cases, the proposed approach could enhance image processing times while maintaining comparable effectiveness.

This research demonstrated the relevance of using free software and open-source technologies for the processing, analysis, and detection of materials in hyperspectral images. Here, the *Spectral* library was used for accessing and extracting information in the form of NumPy arrays corresponding to the reflectance bands of the hyperspectral image. Similarly, the *NumPy* library was highly useful for both obtaining the characteristic pixel of asbestos-cement and implementing the proposed approach utilizing the *fft()* function, which enables the Fourier transform computation of a signal. Additionally, the *Matplotlib* library facilitated the generation of visual representations of the characteristic pixels in different band ranges, along with their Fourier spectral representation. Finally, the *timeit* library allowed evaluating the computational efficiency of the proposed approach in comparison with the correlation method across multiple repetitions. These libraries and technologies are key for the replication and extrapolation of our method in both academic and industrial settings. Compared to proprietary tools, they offer the advantage of customizing and hybridizing material detection methods, enhancing their adaptability and application.

As future work, our approach will be hybridized via the PCA dimensionality reduction method, allowing for an evaluation of its computational efficiency and effectiveness that considers the components with the highest contribution. Similarly, the proposed approach will be evaluated in comparison with machine learning alternatives such as decision tree-based models, which have been effectively used for material detection in hyperspectral images.

ACKNOWLEDGMENTS

This article is a product of the project titled *Formulation of an integral strategy to reduce the impact on public and environmental health due to the presence of asbestos in the territory of the Department of Bolívar*, funded by the General System of Royalties of Colombia (SGR) and identified with the code BPIN 2020000100366. This project was executed by Universidad de Cartagena and the Colombia Libre de Asbesto Foundation. It is also worth mentioning that the dataset used in this article is part of a set of images captured by an aircraft equipped with a spectral sensor, which was funded with project resources.

REFERENCES

Abasova, J., Tanuska, P., & Rydzi, S. (2021). Big data—Knowledge discovery in production industry data storages—Implementation of best practices. *Applied Sciences*, *11*(16), 7648. https://doi.org/10.3390/app11167648

Akinlade, O., Vakaj, E., Dridi, A., Tiwari, S., & Ortiz-Rodriguez, F. (2023). Semantic segmentation of the lung to examine the effect of COVID-19 using UNET model. In M. A. Jabbar, F. Ortiz-Rodríguez, S. Tiwari, & P. Siarry (Dds.), *Applied Machine Learning and Data Analytics. AMLDA 2022*. (Communications in Computer and Information Science, vol. 1818, pp. 52-63). Springer. https://doi.org/10.1007/978-3-031-34222-6_5

Algranti, E., Mendonça, E. M. C., DeCapitani, E. M., Freitas, J. B. P., Silva, H. C., & Bussacos, M. A. (2001). Non-malignant asbestos-related diseases in Brazilian asbestos-cement workers. *American Journal of Industrial Medicine*, *40*(3), 240-254. https://doi.org/10.1002/ajim.1095

Asghari Beirami, B., & Mokhtarzade, M. (2020). Band grouping SuperPCA for feature extraction and extended morphological profile production from hyperspectral images. *IEEE Geoscience and Remote Sensing Letters*, *17*(11), 1953-1957. https://doi.org/10.1109/LGRS.2019.2958833

Awange, J., & Kiema, J. (2019). Fundamentals of remote sensing. In J. Awannge & J. Kiema, *Environmental Geoinformatics* (Environmental Science and Engineering, pp. 115-123). Springer. https://doi.org/10.1007/978-3-030-03017-9_7

Baker, M. (2003). Frequency domain testing and the FFT. In M. Baker, *Demystifying Mixed Signal Test Methods* (pp. 115-146). Elsevier. https://doi.org/10.1016/B978-075067616-8/50005-4

Bassani, C., Cavalli, R. M., Cavalcante, F., Cuomo, V., Palombo, A., Pascucci, S., & Pignatti, S. (2007). Deterioration status of asbestos-cement roofing sheets assessed by analyzing hyperspectral data. *Remote Sensing of Environment*, *109*(3), 361-378. https://doi.org/10.1016/j.rse.2007.01.014

Bonifazi, G., Capobianco, G., & Serranti, S. (2015). *Hyperspectral imaging applied to the identification and classification of asbestos fibers* [Conference article]. *2015 IEEE Sensors*, Busan, South Korea. https://doi.org/10.1109/ICSENS.2015.7370458

Bonifazi, G., Capobianco, G., & Serranti, S. (2018). Asbestos containing materials detection and classification by the use of hyperspectral imaging. *Journal of Hazardous Materials*, *344*, 981-993. https://doi.org/10.1016/j.jhazmat.2017.11.056

Bonifazi, G., Capobianco, G., & Serranti, S. (2019). Hyperspectral Imaging and hierarchical PLS-DA applied to asbestos recognition in construction and demolition waste. *Applied Sciences*, *9*(21), 4587. https://doi.org/10.3390/app9214587

Bonifazi, G., Capobianco, G., Serranti, S., Malinconico, S., & Paglietti, F. (2022). Asbestos detection in construction and demolition waste adopting different classification approaches based on short wave infrared hyperspectral imaging. *Detritus*, *20*, 90-99. https://doi.org/10.31025/2611-4135/2022.15211

Brigham, E. O., & Yuen, C. K. (1978). The fast fourier Transform. *IEEE Transactions on Systems, Man, and Cybernetics*, *8*(2), 146-146. https://doi.org/10.1109/TSMC.1978.4309919

Burger, J., & Gowen, A. (2011). Data handling in hyperspectral image analysis. *Chemometrics and Intelligent Laboratory Systems*, *108*(1), 13-22. https://doi.org/10.1016/j.chemolab.2011.04.001

Chanchí-Golondrino, G. E., Ospina-Alarcón, M. A., & Saba, M. (2024). Fourier analysis for detecting vegetation in hyperspectral images. *Ingeniería y Competitividad*, *26*(3), 13493. https://doi.org/10.25100/iyc.v26i3.13493

Chanchí Golondrino, G. E., Ospina Alarcón, M. A., & Saba, M. (2023). Vegetation identification in hyperspectral images using distance/correlation metrics. *Atmosphere*, *14*(7), 1148. https://doi.org/10.3390/atmos14071148

Durán-Ávila, N. L., Cañarte-Murillo, J. R., Zambrano-Murillo, J. N., & Ayón-Lucio, C. A. (2021). Daño pulmonar causado por asbestos en trabajadores de la construcción. *Cienciamatria*, *7*(1), 260-270. https://doi.org/10.35381/cm.v7i1.529

Enríquez Aguilera, F. J., Silva Aceves, J. M., Torres Argüelles, S. V., Martínez Gómez, E. A., & Bravo Martínez, G. (2018). Utilización de GPU-CUDA en el procesamiento digital de imágenes. *Cultura Científica y Tecnológica*, *66*, 65-79. https://doi.org/10.20983/culcyt.2018.3.9

Fang, Q. (2024). The advantages of using remote sensing technology to monitor forest fires. *Applied and Computational Engineering*, *60*(1), 42-48. https://doi.org/10.54254/2755-2721/60/20240830

Fu, W., Ma, J., Chen, P., & Chen, F. (2020). Remote sensing satellites for Digital Earth. In H. Guo, M. F. Goodchild, & A. Annoni (Eds.), *Manual of Digital Earth* (pp. 55-123). Springer. https://doi.org/10.1007/978-981-32-9915-3_3

Gan, W. S. (2020). Fast Fourier transform. In W. S. Gan (Eds.), *Signal Processing and Image Processing for Acoustical Imaging* (pp. 17-20). Springer. https://doi.org/10.1007/978-981-10-5550-8_5

Gao, L., & Smith, R. T. (2015). Optical hyperspectral imaging in microscopy and spectroscopy - a review of data acquisition. *Journal of Biophotonics*, *8*(6), 441-456. https://doi.org/10.1002/jbio.201400051

Hayat Suhendar, M. T., & Widyani, Y. (2023). *Machine learning application development guidelines using CRISP-DM and scrum concept* [Conference article]. 2023 IEEE International Conference on Data and Software Engineering (ICoDSE), Toba, Indonesia. https://doi.org/10.1109/ICoDSE59534.2023.10291438

Hu, Q., Wang, X., Jiang, J., Zhang, X.-P., & Ma, J. (2024). Exploring the spectral prior for hyperspectral image super-resolution. *IEEE Transactions on Image Processing*, *33*, 5260-5272. https://doi.org/10.1109/TIP.2024.3460470

Jiang, J., Ma, J., Chen, C., Wang, Z., Cai, Z., & Wang, L. (2018). SuperPCA: A Superpixelwise PCA approach for unsupervised feature extraction of hyperspectral imagery. *IEEE Transactions on Geoscience and Remote Sensing*, *56*(8), 4581-4593. https://doi.org/10.1109/TGRS.2018.2828029

Jiang, Z., Chen, J., Chen, J., Feng, L., Jin, M., Zhong, H., Ju, L., Zhu, L., Xiao, Y., Jia, Z., Xu, C., Yu, D., Zhang, X., & Lou, J. (2022). Mortality due to respiratory system disease and lung cancer among female workers exposed to chrysotile in Eastern China: A cross-sectional study. *Frontiers in Oncology*, *12*, 1-10. https://doi.org/10.3389/fonc.2022.928839

Jiménez-López, A. F., Jiménez-López, M., & Jiménez-López, F. R. (2015). Multispectral analysis of vegetation for remote sensing applications. *ITECKNE*, *12*(2), 1242. https://doi.org/10.15332/iteckne.v12i2.1242

Kollar, Z., Plesznik, F., & Trumpf, S. (2018). Observer-Based Recursive Sliding Discrete Fourier Transform [Tips & Tricks]. *IEEE Signal Processing Magazine*, *35*(6), 100-106. https://doi.org/10.1109/MSP.2018.2853196

Krówczyńska, M., Raczko, E., Staniszewska, N., & Wilk, E. (2020). Asbestos-cement roofing identification using remote sensing and convolutional neural networks (CNNs). *Remote Sensing*, *12*(3), 408. https://doi.org/10.3390/rs12030408

Li, S., Song, W., Fang, L., Chen, Y., Ghamisi, P., & Benediktsson, J. A. (2019). Deep learning for hyperspectral image classification: An overview. *IEEE Transactions on Geoscience and Remote Sensing*, *57*(9), 6690-6709. https://doi.org/10.1109/TGRS.2019.2907932

Liu, G., Yang, H., Zhao, H., Zhang, Y., Zhang, S., Zhang, X., & Jin, G. (2021). Combination of structured illumination microscopy with hyperspectral imaging for cell analysis. *Analytical Chemistry*, *93*(29), 10056-10064. https://doi.org/10.1021/acs.analchem.1c00660

Mainieri Hidalgo, J. A., Putvinsky, V., & Mainieri Breedy, G. (2009). Mesotelioma pleural en Costa Rica. *Acta Médica Costarricense*, *48*(1), 217. https://doi.org/10.51481/amc.v48i1.217

Martínez-Plumed, F., Contreras-Ochando, L., Ferri, C., Hernández-Orallo, J., Kull, M., Lachiche, N., Ramírez-Quintana, M. J., & Flach, P. (2021). CRISP-DM twenty years later: From data mining processes to data science trajectories. *IEEE Transactions on Knowledge and Data Engineering*, *33*(8), 3048-3061. https://doi.org/10.1109/TKDE.2019.2962680

Muhammed, S., Rahul, D., & Vishnukumar, S. (2020). Hyperspectral and multispectral image fusion techniques. *International Journal of Recent Technology and Engineering (IJRTE)*, *8*(5), 467-471. https://doi.org/10.35940/ijrte.E4904.018520

Musk, A. W., de Klerk, N., Reid, A., Hui, J., Franklin, P., & Brims, F. (2020). Asbestos-related diseases. *The International Journal of Tuberculosis and Lung Disease*, *24*(6), 562-567. https://doi.org/10.5588/ijtld.19.0645

Nava, J., & Hernández, P. (2012). Optimization of a hybrid methodology (CRISP-DM). In C. A. O Ortiz Zezzatti, C. Chira, A. Hernández, & M. Basurto (Eds.), *Logistics Management and Optimization through Hybrid Artificial Intelligence Systems* (pp. 356-379). IGI Global Scientific Publishing. https://doi.org/10.4018/978-1-4666-0297-7.ch014

Navalgund, R., Jayaraman, V., & Roy, P. (2007). Remote sensing applications: An overview. *Current Science*, *93*, 1747-1766.

Ortega, S., Fabelo, H., Iakovidis, D., Koulaouzidis, A., & Callico, G. (2019). Use of hyperspectral/multispectral imaging in gastroenterology. Shedding some–different–light into the dark. *Journal of Clinical Medicine*, *8*(1), 36. https://doi.org/10.3390/jcm8010036

Ospina, D., Villegas, V. E., Rodríguez-Leguizamón, G., & Rondón-Lagos, M. (2019). Analyzing biological and molecular characteristics and genomic damage induced by exposure to asbestos. *Cancer Management and Research*, *11*, 4997-5012. https://doi.org/10.2147/CMAR.S205723

Plaza, A., Benediktsson, J. A., Boardman, J. W., Brazile, J., Bruzzone, L., Camps-Valls, G., Chanussot, J., Fauvel, M., Gamba, P., Gualtieri, A., Marconcini, M., Tilton, J. C., & Trianni, G. (2009). Recent advances in techniques for hyperspectral image processing. *Remote Sensing of Environment*, *113*, S110-S122. https://doi.org/10.1016/j.rse.2007.07.028

Pollard, J. M. (1971). The fast Fourier transform in a finite field. *Mathematics of Computation*, *25*(114), 365-374. https://doi.org/10.1090/S0025-5718-1971-0301966-0

Ruiz Guzmán, E., Gallegos Rodríguez, A., Flores Garnica, J. G., & Mena Munguía, S. (2024). Aplicación de sensores remotos e inteligencia artificial en la gestión y conservación de bosques frente al cambio climático en México. *E-CUCBA*, *11*(21), 142-149. https://doi.org/10.32870/e-cucba.vi21.332

Sabah Jaber, H. (2018). Classification of hyperspectral remote sensing for production minerals mapping using geological map and geomatics techniques. *International Journal of Engineering & Technology*, *7*(4.20), 480-484. https://doi.org/10.14419/ijet.v7i4.20.26247

Sifnaios, S., Arvanitakis, G., Konstantinidis, F. K., Tsimiklis, G., Amditis, A., & Frangos, P. (2024). *A deep learning approach for pixel-level material classification via hyperspectral imaging*. https://doi.org/10.48550/arXiv.2409.13498

Taiwo, G., Vadera, S., & Alameer, A. (2025). Vision transformers for automated detection of pig interactions in groups. *Smart Agricultural Technology*, *10*, 100774. https://doi.org/10.1016/j.atech.2025.100774

Wang, Z., Ma, Y., Zhang, Y., & Shang, J. (2022). Review of remote sensing applications in grassland monitoring. *Remote Sensing*, *14*(12), 2903. https://doi.org/10.3390/rs14122903

Xing, Y., & Gómez, R. B. (2001). Hyperspectral image analysis using ENVI (environment for visualizing images). In W. E. Roper (Ed.), *Proceedings of SPIE - The International Society for Optical Engineering* (pp. 79-86). SPIE. https://doi.org/10.1117/12.428244

Zhang, X., Jiang, X., Jiang, J., Zhang, Y., Liu, X., & Cai, Z. (2022). Spectral–spatial and superpixelwise PCA for unsupervised feature extraction of hyperspectral imagery. *IEEE Transactions on Geoscience and Remote Sensing*, *60*, 1-10. https://doi.org/10.1109/TGRS.2021.3057701